

## SUPPLEMENTARY FIGURE LEGENDS

**Figure S1. Expression of TDP-43 CTFs in QBI-293 cells also lead to formation of cytoplasmic, hyperphosphorylated aggregates.** (A) Human QBI-293 cells were transfected and analyzed by immunoblot as in Fig 2A. Asterisks indicate the same immunoband in C-t TDP-43 and p409/410 TDP-43 blots. GAPDH was used as a loading control. (B) Double immunofluorescence staining was performed as in Fig. 2C. QBI-293 cells were stained for C-t TDP-43 pAb (green), p409/410 TDP-43 mAb (red) and counterstained with DAPI (blue). The solubility profile and phosphorylation pattern of TDP-43 CTFs in QBI-293 cells was slightly different than that of N2a cells. However there is a similar trend of increased insolubility and aggregation when shorter CTFs are expressed (i.e. 197 TDP-43 and 208 TDP-43). Scale bar = 10  $\mu$ m.

**Figure S2. Myc-tagged TDP-43 CTFs are More Soluble than Untagged Counterpart.**

(A) QBI-293 cells were transfected with vector alone or the different TDP-43 CTFs and 48 hrs later were sequentially extracted with RIPA (R) and urea buffer (U). Immunoblotting was conducted with C-t TDP-43 pAb. GAPDH was used as a loading control. (B) Densitometric analysis of C-t TDP-43 pAb immunoblots shown in (A). Immunobands corresponding to TDP-43 CTFs were quantified and expressed as percentage of RIPA-insoluble/total. There was a significant increase in solubility due to the addition of the myc epitope tag to the N-terminus of the TDP-43 CTFs. Error bars represent S.E.M. \*  $p < 0.05$ ; \*\*  $p < 0.01$ ; \*\*\*  $p < 0.001$  (Student t test, myc-tagged vs untagged for each CTF).

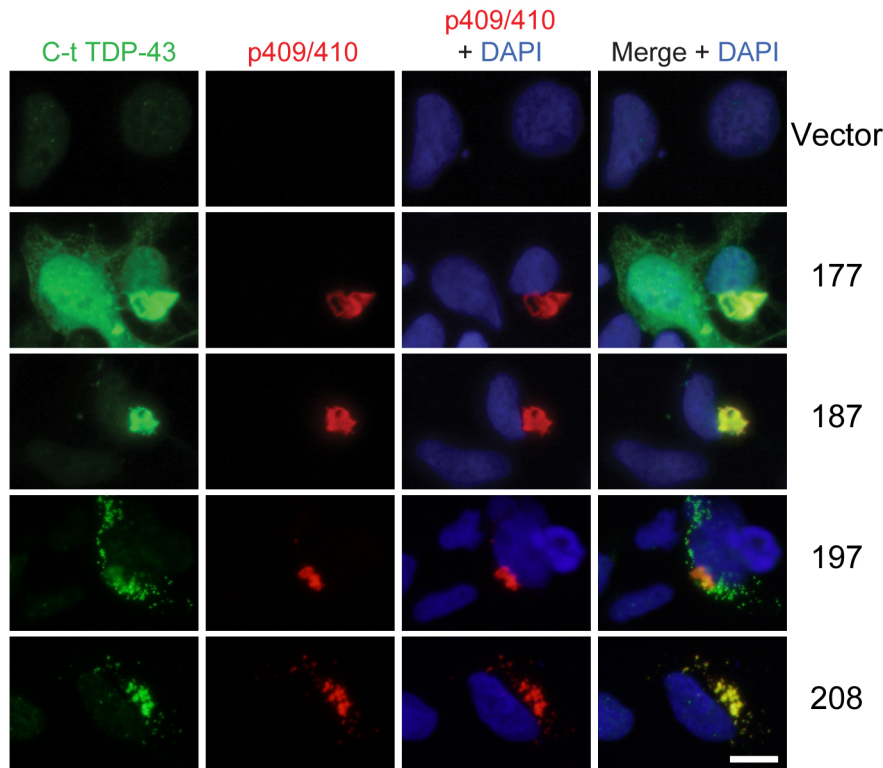
**Figure S3. Quantitative analysis of CFTR Splicing Assay and TDP-43 Protein Levels in transfected QBI-293 Samples.**

(A) Diagram illustrating the workflow of exon splicing experiment. (B) Schematic representation of the previously described hybrid minigene TG13T5 (6). This reporter CFTR-exon 9 construct was used to evaluate the functional impact of TDP-43 expression. Exons are displayed as boxes, and introns as lines, color-coded according to their gene of origin ( $\alpha$ -globin, Fibronectin or CFTR). The TDP-43 binding region, TG(13)T(5) is shown in red. Primers used for the RT-PCR are indicated with the arrows. (C) Representative Agilent electrophoregrams used for quantitative analysis of CFTR minigene splicing, showing peaks corresponding to PCR products including or excluding exon 9. A previously reported aberrant splicing product (6) generated by a cryptic splicing site was revealed as a minor PCR product of intermediate size. Asterisks indicate low and high DNA markers. Note the increase in the exon 9 included peak in TDP-43 CTF samples relative to the vector only sample. (D) C-t TDP-43 immunoblot analysis of the same samples used for the CFTR splicing assay demonstrate robust expression of WT and TDP-43 CTFs, and efficient (>90%) knock-down of endogenous TDP-43 by shRNA treatment. GAPDH was used as a loading control.

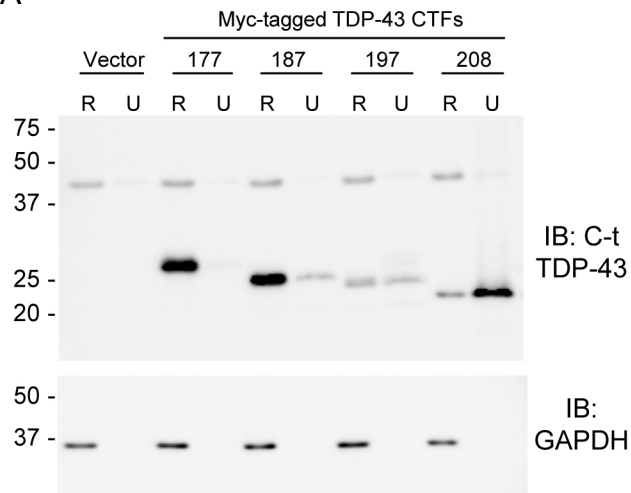
A



B

Supplementary Figure 1 - Igaz *et al.*

A



B

